cosmetics

MDPI

Article

A Novel Development of a *Curcuma aromatica* Salisb Extract-Loaded Hydrogel Patch for Acne and Skin Inflammation: Physicochemical Properties and In Vitro Anti-Inflammatory and Anti-Acne Activities

Chonthicha Kongkwamcharoen [1,2], Suwipa Ungphaiboon [3], Buncha Ooraikul [4] and Chuchard Punsawad [2,5,*]

[1] Department of Applied Thai Traditional Medicine, School of Medicine, Walailak University, Nakhon Si Thammarat 80160, Thailand; chonthicha.kon@wu.ac.th
[2] Center of Excellence in Tropical Pathobiology, Walailak University, Nakhon Si Thammarat 80160, Thailand
[3] Drug Delivery System Excellence Center, Department of Pharmaceutical Technology, Faculty of Pharmaceutical Sciences, Prince of Songkla University, Songkhla 90110, Thailand; suwipa.u@psu.ac.th
[4] Department of Agricultural Food and Nutritional Science, Faculty of Agricultural Life and Environmental Sciences, University of Alberta, Edmonton, AB T6G 2P5, Canada; buncha.ooraikul1@gmail.com
[5] Department of Medical Science, School of Medicine, Walailak University, Nakhon Si Thammarat 80160, Thailand
* Correspondence: chuchard.pu@wu.ac.th

Abstract

Background/Objectives: Inflammatory skin disorders such as dermatitis, psoriasis, and acne that affect patients' quality of life and health require safe and effective active delivery systems. In Thai traditional medicine, *Curcuma aromatica* has long been used to treat skin disorders and for cosmetic skin care. However, the research is scarce. This study aimed to develop and evaluate a novel anti-inflammatory and anti-acne hydrogel patch containing *C. aromatica* extract. **Methods**: The hydrogel patch formulations were prepared, and their mechanical properties, in vitro release, skin permeation, in vitro anti-inflammatory and anti-acne activities, and physicochemical properties were studied. **Results**: The *C. aromatica* hydrogel patch (CA2 formulation) made from carrageenan, locust bean gum, PVP-K30, and *C. aromatica* extract displayed excellent physical appearance and mechanical properties; it was smooth, durable, and flexible. Curcumin, an active ingredient, was released from the *C. aromatica* hydrogel patch within the first 30 min (19.07 ± 1.14%), reaching its peak at 12 h (50.40 ± 3.94%), with sustained permeation of 38.18 ± 0.45% at 24 h. Data from the drug release and permeation study better fit Higuchi's kinetic model. Additionally, the CA2 hydrogel patch demonstrated anti-inflammatory activity, with an IC_{50} value of 19.85 ± 0.82 µg/mL, and was also effective against *Cutibacterium acne*, with an inhibition zone of 12.70 ± 2.10 mm. **Conclusions**: The developed *C. aromatica* hydrogel patch not only showed great physicochemical properties but also had anti-inflammatory and anti-acne activities; it prolonged curcumin release, enabling delivery of the drug to treat skin inflammation disorders. The CA hydrogel patch is suitable for use as an anti-acne facial mask and for inflamed skin areas; however, it should be further evaluated in clinical trials.

Keywords: hydrogel patch; *Curcuma aromatica*; anti-acne; anti-inflammation; curcumin

check for updates

Academic Editor: Enzo Berardesca

Received: 28 August 2025
Revised: 19 October 2025
Accepted: 21 October 2025
Published: 28 October 2025

Citation: Kongkwamcharoen, C.; Ungphaiboon, S.; Ooraikul, B.; Punsawad, C. A Novel Development of a *Curcuma aromatica* Salisb Extract-Loaded Hydrogel Patch for Acne and Skin Inflammation: Physicochemical Properties and In Vitro Anti-Inflammatory and Anti-Acne Activities. *Cosmetics* **2025**, *12*, 240. https://doi.org/10.3390/cosmetics12060240

Copyright: © 2025 by the authors. Licensee MDPI, Basel, Switzerland. This article is an open access article distributed under the terms and conditions of the Creative Commons Attribution (CC BY) license (https://creativecommons.org/licenses/by/4.0/).

1. Introduction

Inflammatory skin disorders including dermatitis, eczema, psoriasis, and acne are common dermatologic illnesses that considerably affect patients' quality of life and health [1,2].

The prolonged release of pro-inflammatory mediators increases transepidermal water loss and compromises skin barrier function, leading to erythema, pruritus, and changes in the epidermal structure [3,4].

Presently, factors such as air pollution and stress can cause inflammation in the body. When stimulated externally, irritation or abnormal immune systems result in an inflammatory process where inflammatory mediators are secreted, resulting in skin inflammation and allergic reactions [5]. Acne has many causes: sebum alteration, aberrant follicular keratinization, *Cutibacterium acnes*, and an inflammatory process [6].

Topical corticosteroids are the most common treatment for inflammatory skin disorders. However, they have side effects, such as redness, thinning of the skin, wilting, and easy bruising [7]. Acne treatments, including retinoids, corticosteroids, and antibiotics, can also cause adverse effects, such as dryness, redness, peeling, and skin irritation [8,9], which can dehydrate the skin and cause inflammation. Thus, our research intends to fill this knowledge gap and find alternative applications that have good anti-inflammatory effects and antibacterial properties but few side effects.

In Thai traditional medicine, the rhizomes of the *Curcuma aromatica* Salisb. (CA) family of Zingiberaceae have long been used to treat inflammatory conditions, wounds, and dermatological skin diseases, in addition to curing bruises, sprains, pain, and swelling [10,11], owing to its anti-inflammatory, antimicrobial, antioxidant, anti-allergic, and wound-healing effects [11–13]. CA powder was traditionally mixed with water or white liquor and applied topically to the affected area, and currently, it is used in spas and skin care; however, few research studies exist. The minimum inhibitory concentration (MIC) of the ethanolic extract and aqueous extract of CA against *C. acnes* was reported to be 125 μg/mL and 250 μg/mL, respectively [14]. In addition, it was reported that CA extract can reduce UVB-induced skin photoaging by reducing MMP-1 expression [15], and that standardized CA extract suppresses colon cancer in vivo [16]. Curcumin is one of the components of curcuminoids, the active compound in CA [17], and has anti-inflammatory effects by inhibiting nitric oxide, IL-1, TNF-α, cox2, and PGE_2 [18], as well as antioxidant, antimicrobial [19], and anti-acne properties [20]. Clinical studies have demonstrated the effect of curcumin in mild to moderate acne [21] and in other dermatological disorders [22]. Therefore, CA is appropriate for use against acne and skin inflammation. However, curcumin is unstable and degrades rapidly at alkaline pH, under high temperatures, and upon exposure to UV or visible light [23,24]. Thus, careful control of pH, temperature, and light is essential for preserving curcumin's integrity in experimental and cosmetic applications.

The topical active delivery system enables precise targeting to the site of action. The most commercial products on the market only come in the form of creams, gels, and lotions, which adhere to clothing and lead to uncontrolled drug release. The patch form, on the other hand, has various advantages: controlled drug release, a low application frequency, prolonged duration of action, convenient use, and portability [25]. Hydrogels, three-dimensional polymer networks with high water-retention capacity, are suitable for inflamed skin, promoting hydration, providing a cooling effect, and reducing redness and heat associated with inflammation [26]. Carrageenan, a polysaccharide from red seaweed, is widely used in cosmetics, foods, and pharmaceuticals due to its excellent gelling ability, swelling capacity, and biocompatibility [27,28]. Locust bean gum (LG) synergistically interacts with carrageenan to improve gel strength, flexibility, and biocompatibility, and thus has potential for wound dressings [29,30]. Polyvinylpyrrolidone K30 (PVP-K30), widely used in pharmaceutics, exhibits excellent film-forming properties [31].

For these reasons, our study aims to develop a novel hydrogel patch containing CA extract for use as an anti-inflammation and anti-acne application, with the objectives of prolonging the duration of action, improving portability, and providing a cooling effect.

In vitro release and skin permeation studies were undertaken using a Franz diffusion cell, and the physicochemical properties of the hydrogel patches were evaluated using scanning electron microscopy (SEM), differential scanning calorimetry (DSC), X-ray diffraction (XRD), and Fourier-transform infrared spectroscopy (FTIR). The anti-inflammatory and anti-*Cutibacterium acnes* activity was assessed by the inhibition of nitric oxide production in LPS-stimulated RAW 264.7 cells and the disc diffusion method, respectively, confirming the patches' effectiveness.

2. Materials and Methods

2.1. Materials and Chemicals

The rhizome of *Curcuma aromatica*, specimen voucher (SKP 206 03 01 01), was collected from Kanchanaburi Province, Thailand, at a latitude of 14°1′ N, longitude of 99°32′ E, and altitude of 29 m. The specimen voucher was placed in the Southern Center of Thai Medicinal Plants at Prince of Songkla University's Faculty of Pharmaceutical Sciences in Thailand. Carrageenan and locust bean gum were purchased from Beauty Cosmetic Co., Ltd., Seoul, Republic of Korea, and PVP K-30 was obtained from the Faculty of Pharmaceutical Sciences, Prince of Songkla University, Thailand. Glycerin was purchased from Sigma-Aldrich (St. Louis, MO, USA), and standard curcumin was purchased from Sigma (St. Louis, MO, USA). Acetonitrile high-performance liquid chromatography (HPLC)-grade was purchased from RCI LabScan (Bangkok, Thailand). The Milli Q® system from Millipore (Bedford, MA, USA) was used to prepare the purified water. The murine macrophage cell line (ATCC® TIB-71™) was Apurchased from the American Type Culture Collection (American Type Culture Collection; ATCC®, Manassas, VA, USA). Sigma (St. Louis, MO, USA) supplied 3-(4,5-dimethyl-2-thiazolyl)-2,5-diphenyl-2H-tetrazolium bromide (MTT).

2.2. Preparation of Extract

The rhizomes of CA were washed, oven-dried at 45 °C, and ground into a coarse powder. The powder (200 g) was macerated with 95% ethanol (500 mL) for three days then filtered through filter paper (Whatman No. 1). The maceration was repeated twice and concentrated at 45–50 °C using a rotary evaporator. The crude extract was stored at –20 °C until use. The yield (%) was calculated as follows:

Yield (%) = (Weight of extract obtained/Total weight of herbal raw material used for extraction) × 100.

2.3. Preparation of CA Hydrogel Patch

Hydrogel patches were prepared by following in Table 1 (Thai Petty Patent Application Number 2503001915). Carrageenan, locust bean gum (LG), PVP K-30 (0.5 g), and glycerin were added step by step and stirred in distilled water until homogeneous. Subsequently, CA extract (1% *w*/*w*) was added and stirred until uniform. The matrix solution was degasified and created the hydrogel patch using a film applicator (3 mm), coated with a polyvinyl chloride (PVC) sheet, and kept in an aluminum foil sealed bag at 4 °C until use.

Table 1. Composition of hydrogel patch formulations (% *w*/*w*).

Formulations	Carrageenan	LG and PVP K-30	Glycerin	*Curcuma aromatica* Extract
B1 (Blank)	1.5	1.5	0.5	-
B2 (Blank)	1.25	1.75	0.5	-
B3 (Blank)	1	2	0.5	-
CA1	1.5	1.5	0.5	1
CA2	1.25	1.75	0.5	1
CA3	1	2	0.5	1

Note: B1–B3 represent blank hydrogel patch formulations (without *Curcuma aromatica* extract), and CA1–CA3 represent *Curcuma aromatica* extract-loaded hydrogel patch formulations.

2.4. Drug Entrapment Efficiency of CA Hydrogel Patches Method

The 95% ethanol was used to dissolve the CA hydrogel patch and sonicated (30 min), and centrifuged at 5000 rpm for 30 min. The supernatant was filtered through a membrane filter prior to curcumin content determination using the HPLC method described in Section 2.6.

2.5. In Vitro Release and Skin Permeation Study

The modified Franz diffusion cell method [32,33] was employed to determine the in vitro release and skin permeation of curcumin from CA hydrogel patches in triplicate.

After soaking in a medium for half an hour, the cellulose dialysis membrane, which has a molecular weight cut-off of 12,000 to 14,000 Da, Cellu Sep T4, Membrane Filtration Product, Inc., USA, was positioned between the donor and receptor compartments. The ethanol (20% *v*/*v*) in the phosphate-buffered saline solution (pH 7.4) was maintained at 37 ± 1 °C and continuously stirred using a magnetic stirrer. The CA hydrogel patch (2 × 2 cm^2) was placed on a cellulose dialysis membrane, and 1 mL aliquots of the receptor medium were withdrawn at predetermined intervals and immediately replenished with an equal volume of fresh medium to maintain sink conditions. Curcumin contents were quantified by high-performance liquid chromatography (HPLC). For the permeation study, excised pig ear skin obtained from Prince of Songkla University (Thailand) was used as the diffusion membrane, and the procedure was performed following the same protocol as the release study.

2.6. HPLC Analytical Method

The HPLC method was validated according to ICH (2005) guidelines [34], assessing parameters such as selectivity, linearity, accuracy, precision, limit of detection (LOD), and limit of quantitation (LOQ). The HPLC system (Dionex Ultimate 3000; Thermo Fisher Scientific, Waltham, MA, USA), C18 column (C18 Hypersil GOLD™, 4.6 × 250 mm), and detector (DAD-3000; Thermo Fisher Scientific, Waltham, MA, USA) were used to analyze the curcumin content. The mobile phase consisted of acetonitrile and 2% (*v*/*v*) acetic acid in DI water at a ratio of 50:50, using an isocratic system. The flow rate was 0.8 mL/min with column temperature at 33 °C, and the running time was 15 min/sample. Ten microliters of each sample were injected into the HPLC system and detected using a diode array detector at a wavelength of 425 nm. The curcumin content was calculated from the standard curve using a linear equation.

2.7. Anti-Inflammatory Activity via Nitric Oxide Inhibition and Cytotoxicity in RAW 264.7 Cells Method

This study used a modified method [35]. RAW 264.7 cells were cultured in DMEM at 37 °C in a 5% CO_2 atmosphere and subsequently seeded into 96-well plates at a density of 1 × 10^5 cells/well. After 24 h, the cells were treated with lipopolysaccharide (LPS) at

5 ng/mL. For testing, each of 1% CA hydrogel patches was prepared at a stock concentration of 50 mg/mL then prepared at various concentrations (5–50 μg/mL). Curcumin standard was prepared at various concentrations (0.1–30 μg/mL). Samples were added to the cells and incubated for 24 h. Thereafter, the supernatant was transferred to a fresh 96-well plate, followed by the addition of Griess reagent. The optical density was then measured at 570 nm using a microplate reader. The viability of the treated cells was determined using MTT solution, and the inhibition and toxicity percentages were calculated. GraphPad Prism software version 10 (San Diego, CA, USA) was used to calculate the half-inhibitory concentration (IC_{50}).

2.8. Determination of Anti-Cutibacterium Acnes Activity of Hydrogel Patch Using Disc Diffusion Method

The anti-*C. acnes* activity of the samples was determined using the disc diffusion method. *C. acnes* (DMST 14916) was cultured in brain–heart infusion (BHI) broth (Difco, BBL™ Bacto™ Brain Heart Infusion) under anaerobic conditions (GasPak™ in a gas jar) at 37 °C for 7 days, and the bacterial suspension was adjusted to a concentration of 10^8 CFU/mL (O.D. 0.1 at 625 nm). BHI agar plates were inoculated by evenly spreading the standardized suspension over the surface. Seven-millimeter patches of CA hydrogel patch (1% CA extract), blank hydrogel patch (without CA extract; negative control), and 0.01% clindamycin hydrogel patch (positive control) were applied to inoculated plates and incubated anaerobically at 37 °C for 7 days. The inhibition zone was measured across the disc (mm) using an antibiotic zone reader (Fisher Scientific Lilly, Bristol, PA, USA).

2.9. Determination of Physicochemical Properties of Hydrogel Patch

2.9.1. pH of Product

The pH of the prepared patch solutions was measured using a calibrated pH meter.

2.9.2. Thickness

The hydrogel patch thickness was measured at three points per hydrogel patch using a Teclock® dial thickness gauge micrometer (n = 3).

2.9.3. Tensile Strength and % Elongation at Break

Tensile strength (kg/cm^2) and percentage elongation at break of the hydrogel patches were measured using a texture analyzer (TA. XT Plus, Stable Micro Systems, Hamilton, MA, USA). Hydrogel patch specimens (1 × 4 cm^2) were secured between two clamps and tested using a 5 kg load cell with a pre-test speed (1 mm/s), test speed (1 mm/s), and trigger force of 5 g. Data were analyzed using the Exponent Lite software version LITE to determine tensile strength and elongation at break (n = 3).

2.9.4. Surface Morphology

The CA2 hydrogel patch and blank hydrogel patch were incubated at 45 °C for 48 h and subsequently attached to a copper shaft and coated with gold using a sputter coater prior to testing. The surface morphology of the hydrogel patches was investigated using an FE-SEM (Field-Emission SEM; Merlin, Zeiss, Dublin, CA, USA) configured with a high voltage of 10 kV.

2.9.5. Differential Scanning Calorimetry (DSC)

The blank hydrogel patch and CA2 hydrogel patch were incubated at 45 °C for 48 h prior to testing. Under a liquid nitrogen, DSC thermograms were performed on a DSC apparatus (DSC 6000, Perkin Elmer (Hopkinton, MA, USA) scanning at a heat flow from 20 °C to 350 °C at a heating rate of 10 °C/min.

2.9.6. X-Ray Diffraction (XRD)

The crystallinity of carrageenan powder, LG powder, PVP-K30 powder, the blank hydrogel patch, and the CA2 hydrogel patch was investigated using XRD (model: Bruker AXS Model D8 Advance, Karlsruhe, Germany). Both hydrogel patches were incubated at 45 °C for 48 h prior to testing. The conditions were set as follows: X-ray source of 40 mA; voltage of 40 kV; increments of 0.02 degree/step; and angle (2θ) range of 5–40°.

2.9.7. FTIR Spectroscopy

CA, standard curcumin, carrageenan, LG, PVP-K30 powder, the blank hydrogel patch, and the CA2 hydrogel patch were all analyzed using an FTIR spectrometer (Nicolet iS50, Thermo Scientific, USA). Before testing, the blank and CA2 hydrogel patches were incubated at 45 °C for 48 h. The test included 64 scans at a resolution of 4 cm^{-1} and a wave number range from 4000 to 400 cm^{-1} [35].

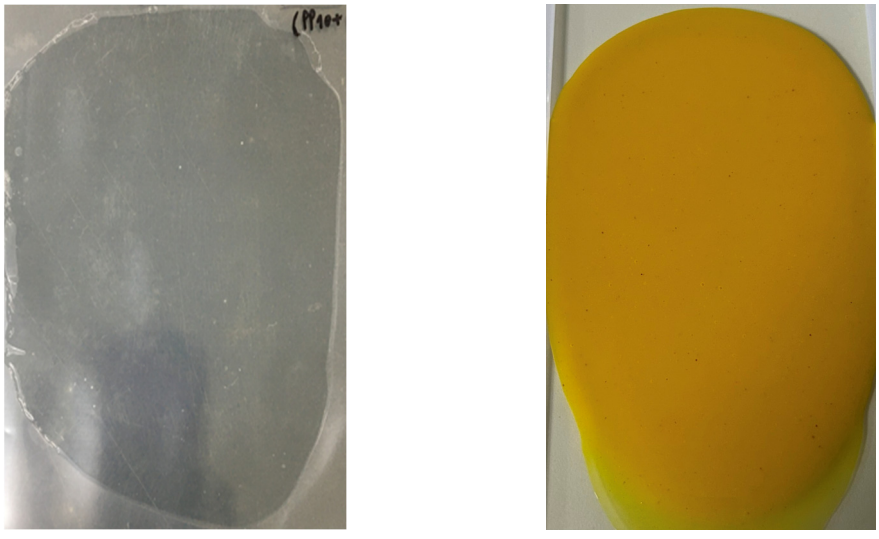
2.10. Statistical Analysis

All data are the mean of three replications, and the values of the hydrogel patches' anti-inflammatory activity parameters is expressed as mean ± SEM. Mechanical and physicochemical properties, and anti-acne activity against *C. acnes* using the disc diffusion method are expressed as mean ± SD, as are those of the in vitro release and skin permeation. The Prism software version 10 was used to determine the IC_{50} values. Tukey's multiple comparison tests and one-way ANOVA were used to examine the data. $p < 0.05$ was considered statistically significant.

3. Results and Discussion

3.1. C. aromatica Extract and Physical Appearance of Hydrogel Patch

The CA ethanolic extract had a yellow–orange color, and its yield percentage was 18.26% (*w*/*w*). The blank hydrogel patch was clear and colorless, and the CA hydrogel patch was yellow (Figure 1). The yellow color of the CA hydrogel, due to curcumin, confirms that the extract was fully loaded and compatible with the hydrogel matrix, forming a smooth, uniform surface that is both suitable and visually appealing for use. However, the yellow color may cause skin staining.



(**a**) (**b**)

Figure 1. The physical appearance of hydrogel patches: (**a**) blank hydrogel patch (without *C. aromatica* extract); (**b**) CA hydrogel patch (hydrogel loaded with *C. aromatica* extract).

3.2. Mechanical and Physicochemical Properties of Hydrogel Patches

The mechanical and physicochemical properties of six formulations are shown in Table 2. The thickness of the blank hydrogel patches (B1–B3) varied between 0.59 ± 0.01 and 0.63 ± 0.01 mm, and the thickness of the CA hydrogel patches varied between 0.57 ± 0.02 and 0.63 ± 0.03 mm, indicating a slight decrease in thickness when adding CA, but one that is not significant within the same formula.

Table 2. Results of mechanical and physicochemical properties of hydrogel patches (mean ± SD).

Formulation	Thickness (mm) ± SD	pH Value ± SD	Tensile Strength (kg/cm^2) ± SD	Elongation at Break (%) ± SD
B1	0.63 ± 0.01	6.83 ± 0.31	1.21 ± 0.13	209.41 ± 4.90
B2	0.59 ± 0.01	6.80 ± 0.26	1.14 ± 0.21	242.65 ± 7.95
B3	0.61 ± 0.01	6.83 ± 0.29	1.20 ± 0.18	269.00 ± 5.52
CA1	0.63 ± 0.03	5.58 ± 0.10 *	1.52 ± 0.13 *	199.75 ± 13.37
CA2	0.57 ± 0.02	5.57 ± 0.12 *	1.50 ± 0.09 *	264.15 ± 19.08
CA3	0.60 ± 0.01	5.57 ± 0.12 *	1.46 ± 0.12	285.02 ± 18.56

B1–B3 indicate blank hydrogel patches (without *C. aromatica* extract); CA1–CA3 indicate hydrogel patches (hydrogel loaded with *C. aromatica* extract) * A significant difference ($p < 0.05$) was observed between the blank hydrogel patch and the CA hydrogel patch; CA, *Curcuma aromatica*.

The pH values of the CA hydrogel patch, at 5.57–5.58, were significantly lower ($p < 0.05$) than those of the blank hydrogel patches, indicating the acidity of the CA extract. The human skin surface is considered to have an acidic nature, with a pH of 4.1–5.8 [36], which is beneficial for epidermal physiology and cutaneous microbiota, and especially cosmetic-relevant skin conditions and skin disorders. Skin care products with a pH level of 4.0–5.5 help to maintain the skin's protective barrier and prevent irritation and dryness [37–39]. Thus, the pH of CA hydrogel patches is suitable for use in skin.

The tensile strength values of blank hydrogel patches (B1–B3) ranged from 1.14 ± 0.21 kg/cm^2 to 1.21 ± 0.13 kg/cm^2, whereas those of CA hydrogel patches (CA1–CA3) ranged from 1.46 ± 0.12 kg/cm^2 to 1.52 ± 0.13 kg/cm^2.

The elongation at break (%) values of blank hydrogel patches (B1–B3) ranged from 209.41 ± 4.90 to 269.00 ± 5.52%, while those of CA hydrogel patches (CA1–CA3) ranged from 199.75 ± 13.37 to 285.02 ± 18.56%. These results show that, when the CA extract is added to the hydrogel, the tensile strength and % elongation at break values slightly increase, indicating that some phytochemicals of CA may interact, favorably forming hydrogen bonds with polymers and enhancing mechanical strength. These findings have been observed in other medicinal plant-loaded hydrogels, where they increased flexibility [40,41].

In our study, the CA hydrogel patch was made from biodegradable polymers such as carrageenan and LG, which are widely used in cosmetics, food, and pharmaceuticals [42,43]. The synergistic interaction between carrageenan and LG enhanced the hydrogel forming and strength [44,45]. Glycerin was used as a plasticizer, increasing the hydrogel patch's flexibility [46].

CA-loaded hydrogel patches demonstrate improved mechanical strength, resilience, and a favorable skin-acidic pH profile, making them strong candidates for effective, user-friendly active delivery systems.

3.3. Drug Entrapment Efficiency of CA Hydrogel Patches

The curcumin entrapment efficiency of hydrogel patches was analyzed using the HPLC method, and was determined as 93.78 ± 2.64, 91.49 ± 1.39, and 86.78 ± 1.60% for the CA2, CA3, and CA1 hydrogel patches, respectively. The CA2 hydrogel formula resulted in

the highest percentage of curcumin loaded relative to the amount initially incorporated and released from the hydrogel matrix.

3.4. In Vitro Drug Release Study

The release profiles of all formulations of the CA1 (high proportion of carrageenan), CA3 (high proportion of LG), and CA2 hydrogel patches (1:1 ratio of carrageenan–LG) exhibit a gradual and sustained release of curcumin over a 12 h period (Figure 2). A rapid initial release phase is observed within the first 30 min at 15–22% for all formulations, indicating a burst release, which is beneficial for use as a mask hydrogel, whereas the profiles between 2 and 6 h suggest controlled diffusion from the matrix.

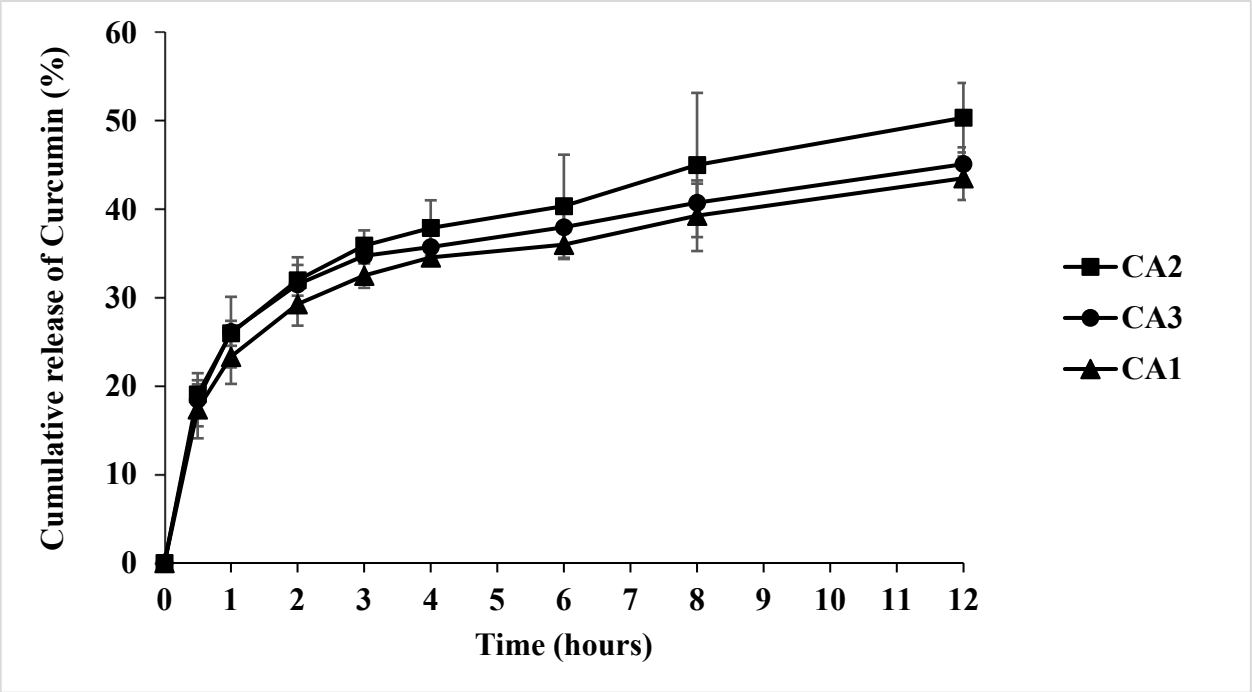


Figure 2. The in vitro cumulative release of curcumin (%) from CA1, CA2, and CA3 hydrogel patches using a modified Franz diffusion cell.

The CA2 hydrogel patch exerted the highest cumulative curcumin release at 12 h, with 50.40 ± 3.94%, while the CA3 and CA1 hydrogel patches reached 45.15 ± 1.90% and 43.55 ± 2.46%, respectively. The effect of the polymer proportion on curcumin release was evident in this study: formulations CA1 (high proportion of carrageenan) and CA3 (high proportion of LG) exhibited lower cumulative curcumin release. This may be attributed to the higher contents of carrageenan and LG, which increase the structural rigidity of the hydrogel patch, potentially reducing its solubility and thereby limiting drug release. Our results are in line with the previous research study by Kaur et al., in which an increase in the concentrations of LG and montmorillonite resulted in a reduced release of curcumin from κ-carrageenan/locust bean gum/montmorillonite composite films [47].

According to Table 3, Higuchi's model was best fitted with the CA2 hydrogel patch's release kinetics model (R^2 = 0.9147). Furthermore, the sustained release of curcumin is advantageous for a prolonged duration of action.

Table 3. Study of the kinetic models of CA hydrogel patches upon release.

Hydrogel Patches	Zero Order $Q_t = K_0t + Q_0$	First Order $(Q_t = Q_0e^{-Kt})$	Higuchi $(Q_t = K_H\sqrt{t})$
	R^2	R^2	R^2
CA1	0.6524	0.7321	0.8890
CA2	0.6951	0.7948	0.9147
CA3	0.6200	0.7037	0.8650

3.5. Anti-Inflammatory Activity via Nitric Oxide Inhibition and Cytotoxicity in RAW 264.7 Cells

As shown in Figure 3, *C. aromatica* (CA) extract demonstrated strong inhibitory activity, with an IC_{50} value of 14.25 ± 1.29 μg/mL. Curcumin showed high activity, with an IC_{50} value of 4.91 ± 0.46 μg/mL, and prednisolone, the positive control, exerted inhibitory activity, with an IC_{50} value of 1.13 ± 0.16 μg/mL. However, if used as a topical drug for a long duration, side effects such as steroid acne, steroid-addicted skin, thinning skin, stretch marks, easy bleeding, and red skin emerged [48].

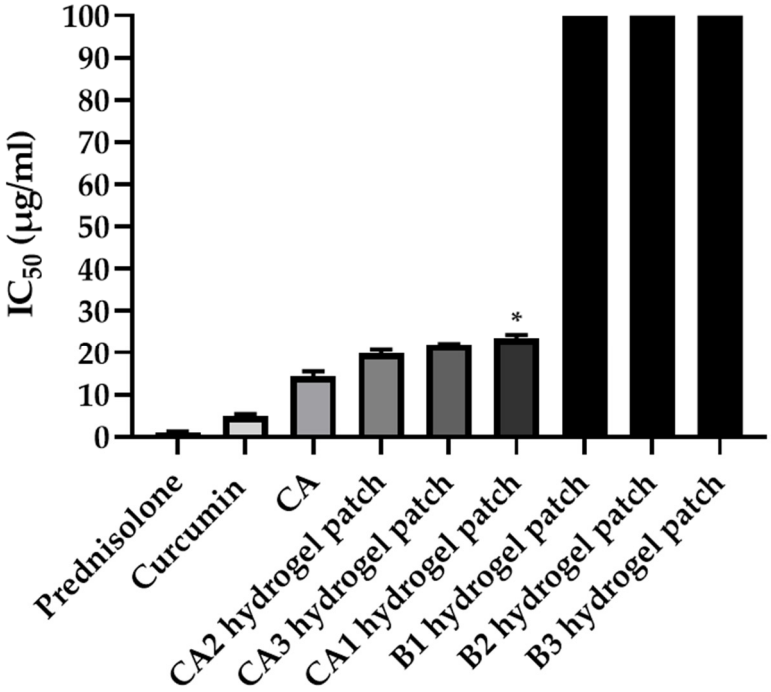


Figure 3. Anti-inflammatory activity via nitric oxide inhibition in RAW 264.7 cells; the IC_{50} values (μg/mL) of prednisolone (positive control), curcumin, CA extract, CA hydrogel patch formulations (CA1–CA3), and blank hydrogel patch formulations (B1–B3). * Significant difference ($p < 0.05$) when compared with CA2 hydrogel patch in groups of CA hydrogel patch (CA1–CA3) analyzed by Tukey's multiple comparisons test.

Regarding the CA1, CA2, and CA3 hydrogel patches, the CA2 hydrogel patch showed the strongest inhibitory activity, with an IC_{50} value of 19.85 ± 0.82 μg/mL, followed by the CA3 and CA1 hydrogel patches, with IC_{50} values of 22.00 ± 0.17 and 23.48 ± 0.92 μg/mL, respectively, while the blank hydrogel patch (B1-B3) did not inhibit nitric oxide production. These results indicate that the anti-inflammatory activity of the CA hydrogel patch is derived directly from *C. aromatica* extract, not from the hydrogel base. In addition, the anti-inflammatory activity of the CA2 hydrogel patch was similar to that of the *C. aromatica* extract, indicating that the hydrogel base neither interferes with nor diminishes the bioactivity of the extract.

In the comparison of anti-inflammatory activity among CA hydrogel patches (CA1–CA3), the best formula was the CA2 hydrogel patch. These results are consistent with drug entrapment efficiency, with a higher entrapment correlating with distinct release behavior and anti-inflammatory activity. A previous research study reported the potential of the crude extract of *C. aromatica* and curcumin to inhibit NF-κB activity [49]. In addition, the extracts of *C. aromatica* showed anti-inflammatory activity in an in vivo study, orally administered to mice, suppressing IL-6, TNF-α, and IL-1β expression [50], and curcumin also showed anti-inflammatory activity [51]. These previous reports are in line with the anti-inflammation of CA and curcumin indicated in our results; however, our results demonstrate the first report of anti-inflammatory activity by the inhibition of nitric oxide production and cytotoxicity on RAW 264.7 cells.

Cytotoxicity was determined using an MTT assay: curcumin showed toxicity at concentrations greater than 20 μg/mL, while CA hydrogel patches were not toxic at all concentrations. Therefore, our study demonstrates that the CA hydrogel patch has anti-inflammatory activity and is not toxic to cells.

3.6. Anti-Acne Activity Against Cutibacterium Acnes of Hydrogel Patch

The anti-*Cutibacterium acnes* activity of various hydrogel patch formulations was evaluated using the disc diffusion method (Table 4 and Figure 4). The CA2 hydrogel patch exerted the strongest activity, with an inhibition zone of 12.70 ± 2.10 mm, followed by the CA3 and CA1 hydrogel patches, with inhibition zones of 11.20 ± 1.10 and 9.60 ± 0.50 mm. The difference in inhibition zones between the CA1 and CA2 hydrogel patches was significant ($p < 0.05$). The blank hydrogel patch formulations (B1, B2, and B3) exhibited no activity against *C. acnes*, indicating that the CA hydrogel patches' anti-*C. acnes* effect was derived directly from the CA extract. In agreement with a previous study reported that the ethanolic extract of CA demonstrated activity against *C. acnes*, with an MIC of 125 μg/mL [14].

The 0.01% clindamycin hydrogel patch (positive control) exhibited a significantly larger inhibition zone of 29.10 ± 1.80 mm. Although the 0.01% clindamycin hydrogel patch demonstrated greater inhibition than the CA2 hydrogel patch, it also resulted in adverse effects such as dry, itchy, irritated, and red skin [52]. Our results show that adding CA ethanolic extract at a concentration of 1% *w*/*w* to the hydrogel patch was sufficient for inhibiting *C. acnes*.

Table 4. Anti-acne activity of hydrogel patch against *C. acnes* using the disc diffusion method.

Samples	Code	Inhibition Zone (mm; Mean ± SD, *n* = 6)
CA1 hydrogel patch 1%	CA1	9.60 ± 0.50 *
CA2 hydrogel patch 1%	CA2	12.70 ± 2.10
CA3 hydrogel patch 1%	CA3	11.20 ± 1.10
B1 hydrogel patch	B1	NA
B2 hydrogel patch	B2	NA
B3 hydrogel patch	B3	NA
Clindamycin hydrogel patch 0.01%	Clindamycin 0.01%	29.10 ± 1.80
Commercial anti-acne patch product; Salicylic acid 0.4% patch	CS	0.00 ± 0.00
Commercial anti-acne patch product; Acne-absorbing patch	CM	0.00 ± 0.00

NA means no inhibition zone. * Significant difference ($p < 0.05$) when compared with CA2 hydrogel patch in CA hydrogel patch groups (CA1–CA3) analyzed by Tukey's multiple comparisons test.

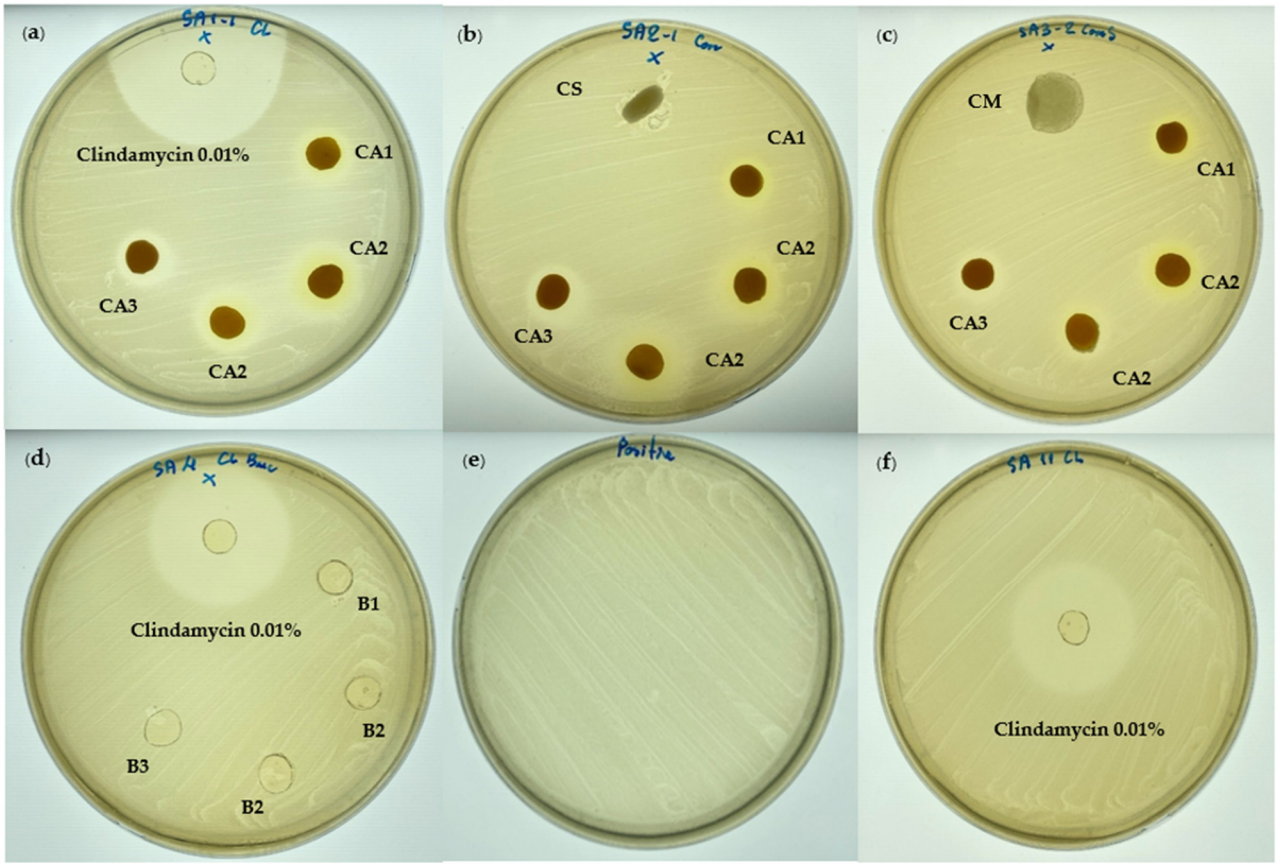


Figure 4. The anti-acne activity of the CA hydrogel patch against *C. acnes* using the disc diffusion method: (**a**) CA hydrogel patches (CA1, CA2, CA3) and 0.01% clindamycin hydrogel patch (positive control); (**b**) CA hydrogel patches (CA1, CA2, CA3) and CS (commercial anti-acne patch product; salicylic acid 0.4% patch); (**c**) CA hydrogel patches (CA1, CA2, CA3) and CM (commercial anti-acne patch product; acne-absorbing patch); (**d**) blank hydrogel patches (B1, B2, B3) and 0.01% clindamycin hydrogel patch (positive control); (**e**) control *C. acnes* (DMST 14916); (**f**) 0.01% clindamycin hydrogel patch (positive control).

Regarding commercial anti-acne patch products, the salicylic acid 0.4% patch (CS) and commercial acne-absorbing patch (CM) showed no inhibition against *C. acnes*. Although salicylic acid has comedolytic and bactericidal properties for acne patients [53], the salicylic acid 0.4% patch (CS) showed no inhibition against *C. acnes* in this study due to the low concentration (0.4%) and its mode of action, which is primarily keratolytic rather than bactericidal. The commercial acne-absorbing patch (CM) also showed no inhibition, potentially due to its mechanism focusing on fluid absorption and wound protection rather than antimicrobial action.

Thus, the CA2 hydrogel patch demonstrated in vitro anti-inflammatory and anti-acne activities, and strong anti-acne activity against *C. acnes* using the disc diffusion method rather than commercial anti-acne patch products. In addition, hydrogel patches provide moisture to the inflamed area and can also absorb fluids due to the hydrogel's properties [54,55]. To our knowledge, this is the first report on the development of a hydrogel patch delivery platform incorporating *C. aromatica* extract, highlighting its potential as a novel anti-acne and anti-inflammatory application for acne and skin disorders.

3.7. In Vitro Skin Permeation Study

The in vitro skin permeation study of the CA2 hydrogel patch was carried out using a modified Franz diffusion cell. As shown in Figure 5, at 3 h, the CA2 hydrogel patch demon-

strated initial curcumin permeation of 28.62 ± 0.45%; moreover, at 24 h, it demonstrated the maximum cumulative curcumin permeation of 38.18 ± 0.45%. The skin permeation kinetics model of the CA2 hydrogel patch better fit Higuchi's model, with R^2 = 0.7011 (Table 5). Glycerin, which was used as a plasticizer in our study, could act as a penetration enhancer, increasing the permeability of curcumin from the CA2 hydrogel patch to the skin [56]. This result confirms that the active compound curcumin efficiently penetrates the skin from the CA2 hydrogel patches. However, approximately 62% of curcumin remained on the skin surface, providing continued topical activity and prolonged topical efficacy. For acne, the effective target is local action (epidermis/follicle). These properties make it suitable for use in skin applications or as a hydrogel mask, where the results suggest that it could be applied directly for dermatological purposes or further adapted for other applications. These findings provide supportive evidence and serve as valuable preliminary data.

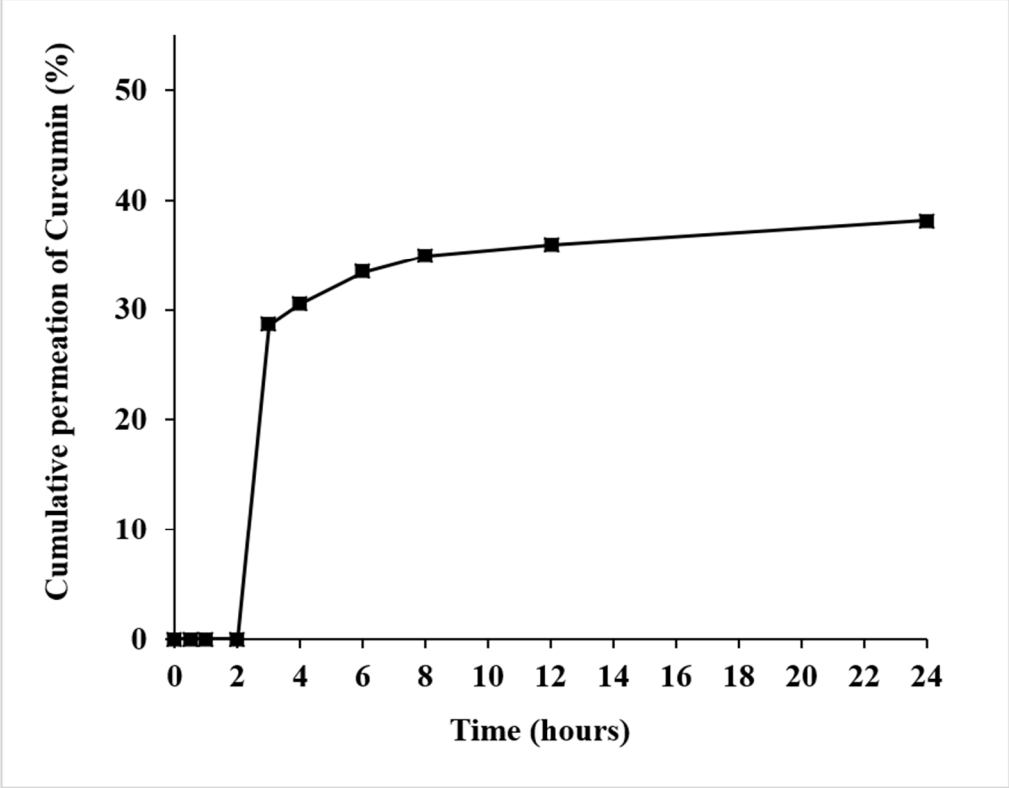


Figure 5. The skin permeation (in vitro) of curcumin from the CA2 hydrogel patch using a modified Franz diffusion cell containing 20% *v*/*v* ethanol in phosphate-buffered saline.

Table 5. The kinetic models of CA2 hydrogel patches in the permeation study.

Hydrogel Patch	Zero Order $Q_t = K_0t + Q_0$	First Order (Q_t Q_0e^{-Kt})	Higuchi ($Q_t = K_H \sqrt{t}$)
	R^2	R^2	R^2
CA2	0.4957	0.4763	0.7011

3.8. Physicochemical Properties of the Hydrogel Patch

3.8.1. The Surface Morphology

The surface morphology of the blank hydrogel patch and the CA2 hydrogel patch was determined using SEM. As shown in Figure 6A (100×) and Figure 6B (500×), the surface of the blank hydrogel patch exhibited a smooth and continuous surface without visible pores or disruptions, suggesting a uniform polymeric matrix. The surface of the CA2

hydrogel patch (Figure 6C at 100× and Figure 6D at 500×) showed several vesicles in the matrix, indicating that *C. aromatica* extract presented distinct spherical domains dispersed throughout it. These results support that *C. aromatica* extract is completely loaded and evenly distributed in the hydrogel patch matrix.

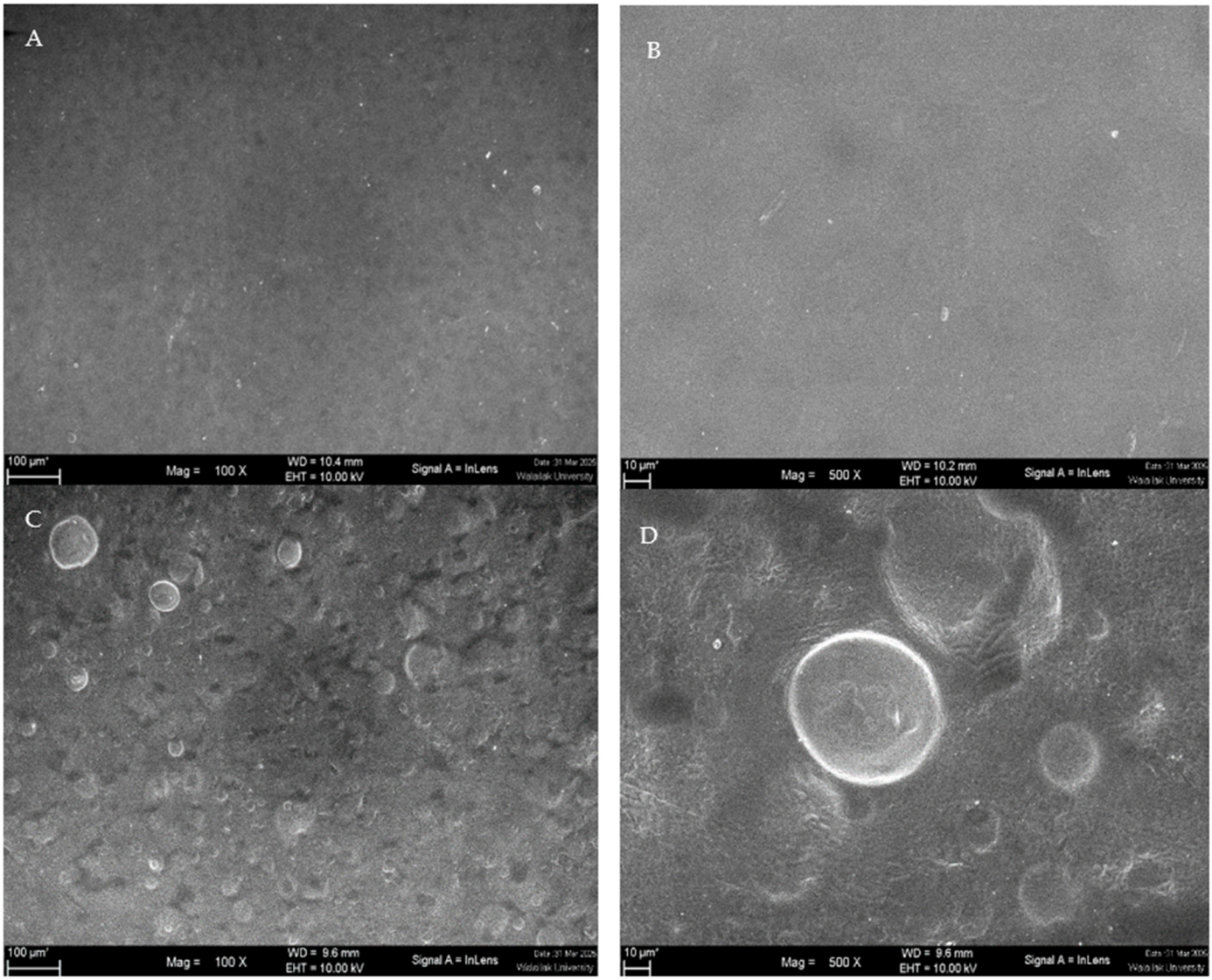


Figure 6. Surface morphology of hydrogel patch: (**A**) surface morphology of a blank hydrogel patch ×100; (**B**) ×500; (**C**) the surface morphology of the CA2 hydrogel patch ×100; (**D**) ×500.

3.8.2. Differential Scanning Calorimetry Analysis

The DSC thermograms of the CA2 hydrogel patch, blank hydrogel patch, carrageenan powder, LG powder, and PVP-K30 powder are displayed in Figure 7. The DSC thermogram of LG powder exhibited a broad endotherm peak at 90.06 °C and melting point at 191.69 °C, whereas that of carrageenan powder showed an endothermic peak at 97.35 °C, corresponding to the melting of its crystalline regions, a melting point at 151.43 °C, and an exothermic peak at 207.99 °C, indicative of its thermal degradation caused by the fragmentation of the polymeric backbone [57]. This finding aligns with a prior study, where carrageenan exerted exothermic peaks at 239 °C [58]. The DSC thermogram of PVP-K30 demonstrated a characteristic broad thermal transition near 88.56 °C, associated with water loss.

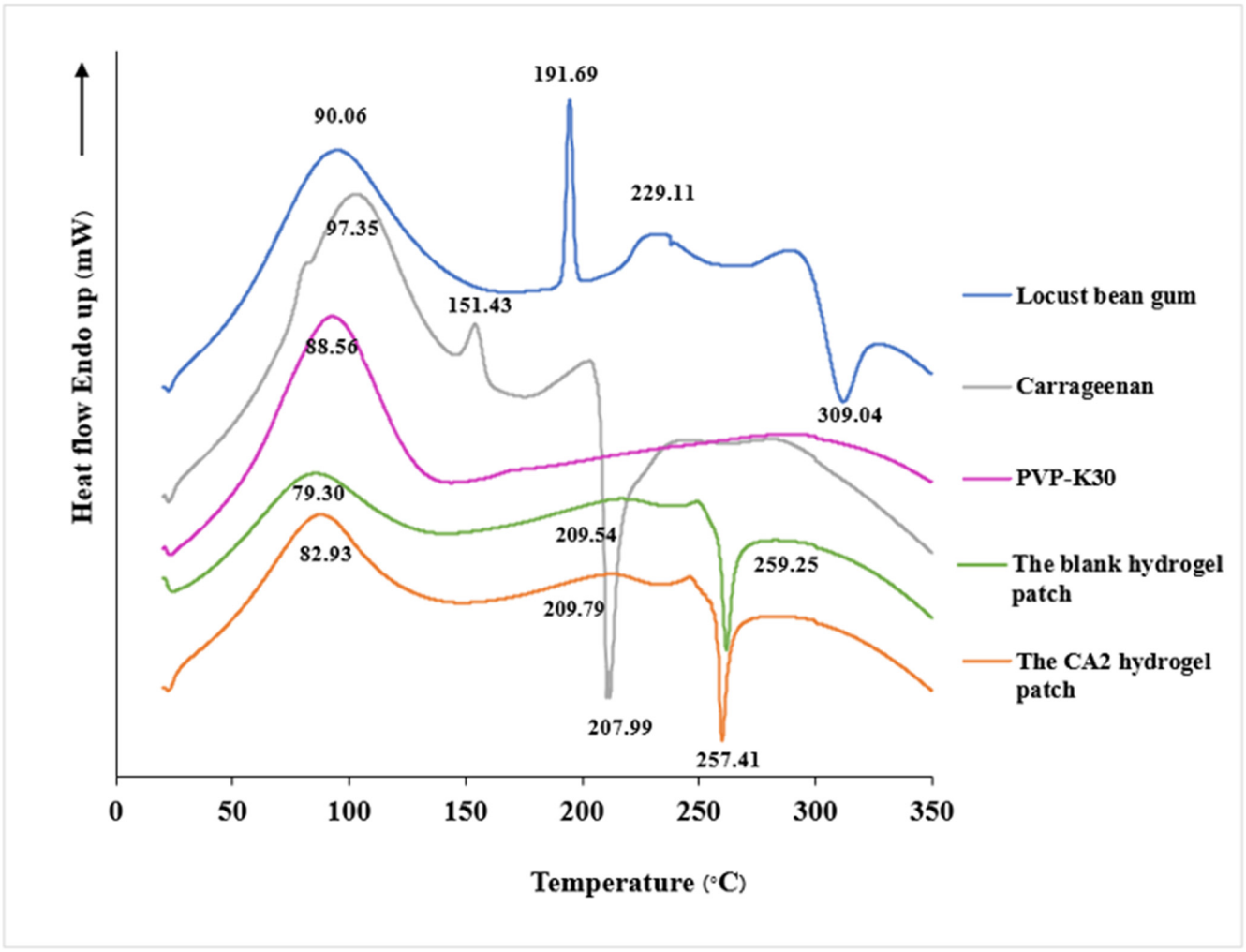


Figure 7. DSC thermograms of LG powder, carrageenan powder, PVP-K30, the blank hydrogel patch, and the CA2 hydrogel patch.

The analysis thermogram of the blank hydrogel patch revealed an endothermic peak at 79.30 °C, which is similar to those of pure carrageenan, LG, and PVP-K30. The melting point was 209.54 °C. The CA2 hydrogel patch exhibited high broad endothermic peaks at 82.93 °C and 209.79 °C. The DSC thermograms of both the blank and CA2 hydrogel patches showed no additional thermal events, indicating the absence of significant chemical interactions or incompatibilities among the components. This thermal compatibility is crucial for the stability and efficacy of the hydrogel formulation. The thermal analysis results also showed that the CA2 hydrogel patch maintained thermal stability up to 250 °C and is hence suitable for cosmetic/skin care applications.

3.8.3. XRD Analysis

The blank hydrogel patch's XRD pattern showed amorphous characteristics, with a broad diffraction region at 10° and 20° (2θ) and no sharp peaks. The XRD pattern of the CA2 hydrogel patch also showed amorphous characteristics, with a large diffraction region at 20° (2θ) and no crystalline peaks (Figure 8).

Consequently, the XRD pattern of the CA2 hydrogel patch confirmed its amorphous nature, indicating that curcumin was completely dispersed within the hydrogel matrix. Furthermore, amorphous regions led to enhanced drug diffusion [59].

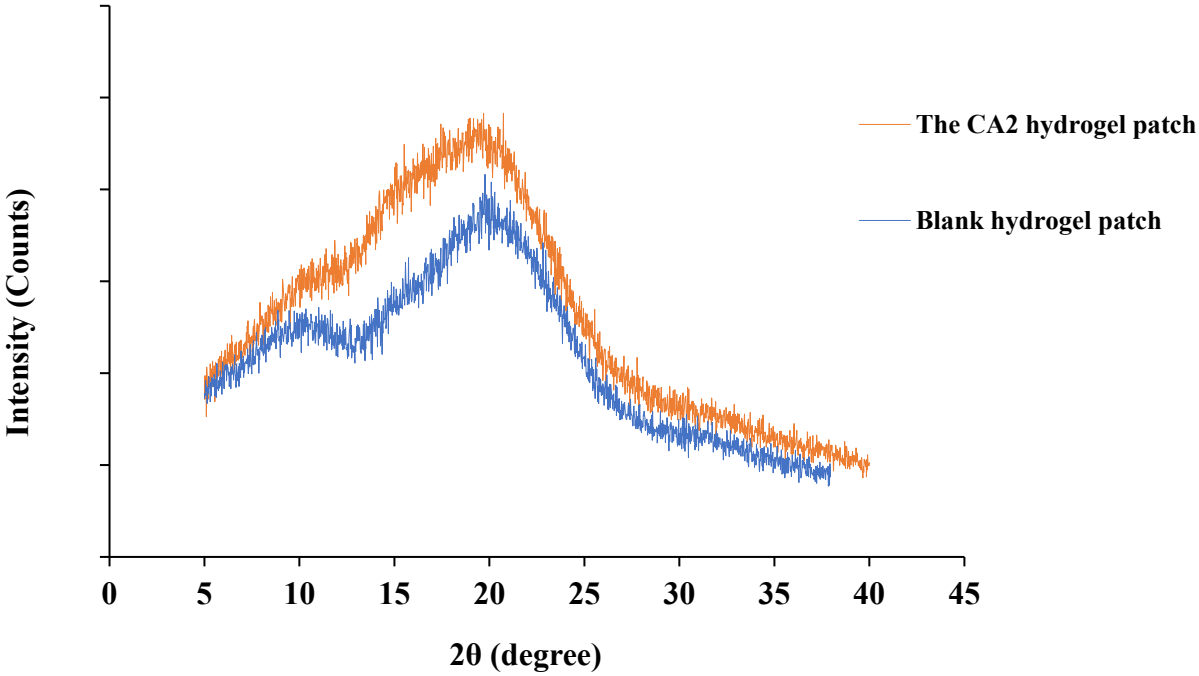


Figure 8. The XRD patterns of the CA2 hydrogel patch and blank hydrogel patch.

3.8.4. FTIR Analysis

The FTIR spectra of curcumin, *Curcuma aromatica* extract, the CA2 hydrogel patch, the blank hydrogel patch, carrageenan, LG, and PVP-K30 are shown in Figure 9. The spectrum of the blank hydrogel patch demonstrated characteristic absorption bands, including a broad O–H stretching vibration at 3300–3400 cm^{-1}, C–H stretching in the range of 2900–3000 cm^{-1}, and ester sulfate groups at 1220–1223 cm^{-1}, which is similar to the spectrum of carrageenan (1221.45 cm^{-1}), indicating that ester sulfate moieties are an inherent structural component of carrageenan [45]. The FTIR spectrum of LG exhibited a broad O–H stretching vibration at 3329.08 cm^{-1} and an aliphatic C–H stretching band at 2890.22 cm^{-1}, consistent with characteristic functional groups commonly found in polysaccharides. Evidence of chemical interaction between carrageenan and LG is supported by a noticeable shift in the C–O stretching vibration of the C–O–H functional group. Specifically, the peak at 1155.80 cm^{-1} observed in pure carrageenan was shifted to 1150.87 cm^{-1} in the spectrum of the blank hydrogel patch. This shift suggests potential hydrogen bonding intermolecular interactions between carrageenan and LG [47].

The FTIR spectrum of PVP-K30 revealed a strong and sharp band at 1614.99 cm^{-1} attributed to the C=O stretching of the pyrrolidone ring, similar to previous research [60,61]. A broad O–H band centered at 3411.32 cm^{-1} and a C–H stretching peak at 2950.79 cm^{-1} were also observed, both typical for hygroscopic polymer systems. These peaks remained visible in both the blank and CA2 hydrogel patches, implying that the physical structure of PVP-K30 was retained post-formulation.

The FTIR spectrum of curcumin exhibited characteristic bands at 3507.29 cm^{-1}, attributable to O–H stretching vibrations arising from phenolic hydroxyl groups. The aromatic C=C stretching (1626.33 cm^{-1}), benzene ring stretching vibrations (1600–1605 cm^{-1}), and C=O stretching (1500–1515 cm^{-1}) determined were similar to previous research [62,63].

The FTIR spectrum of the *C. aromatica* extract showed a slight shift in the O–H band to 3475.12 cm^{-1} and C=O/C=C stretching to 1658.75 cm^{-1}, along with an additional band at 1513.66 cm^{-1} from curcumin, suggesting the presence of other phytoconstituents in the extract that may influence the vibrational environment. However, it also demonstrated characteristic bands at 1658.75 and 1513.66 cm^{-1}, closely matching the spectrum of cur-

cumin (at 1626.33 and 1505.57 cm^{-1}), thereby suggesting the presence of curcumin in the extract.

The FTIR spectrum of the CA2 hydrogel patch exhibited key absorption bands at 3330.70 cm^{-1} (O–H stretching) and 2925.85 cm^{-1} (C–H stretching), confirming the hydrophilic polymeric nature of the matrix. Importantly, the C=O stretching peak observed in the CA extract (1658.75 cm^{-1}) was retained in the CA2 hydrogel patch at 1652.79 cm^{-1}. Moreover, the aromatic C=C band was preserved at 1513.85 cm^{-1}. Its characteristic bands were close to those in the spectrum of the curcumin and extract, indicating that curcumin, an active marker of the CA extract, was completely dispersed in the hydrogel patch matrix without significant structural degradation.

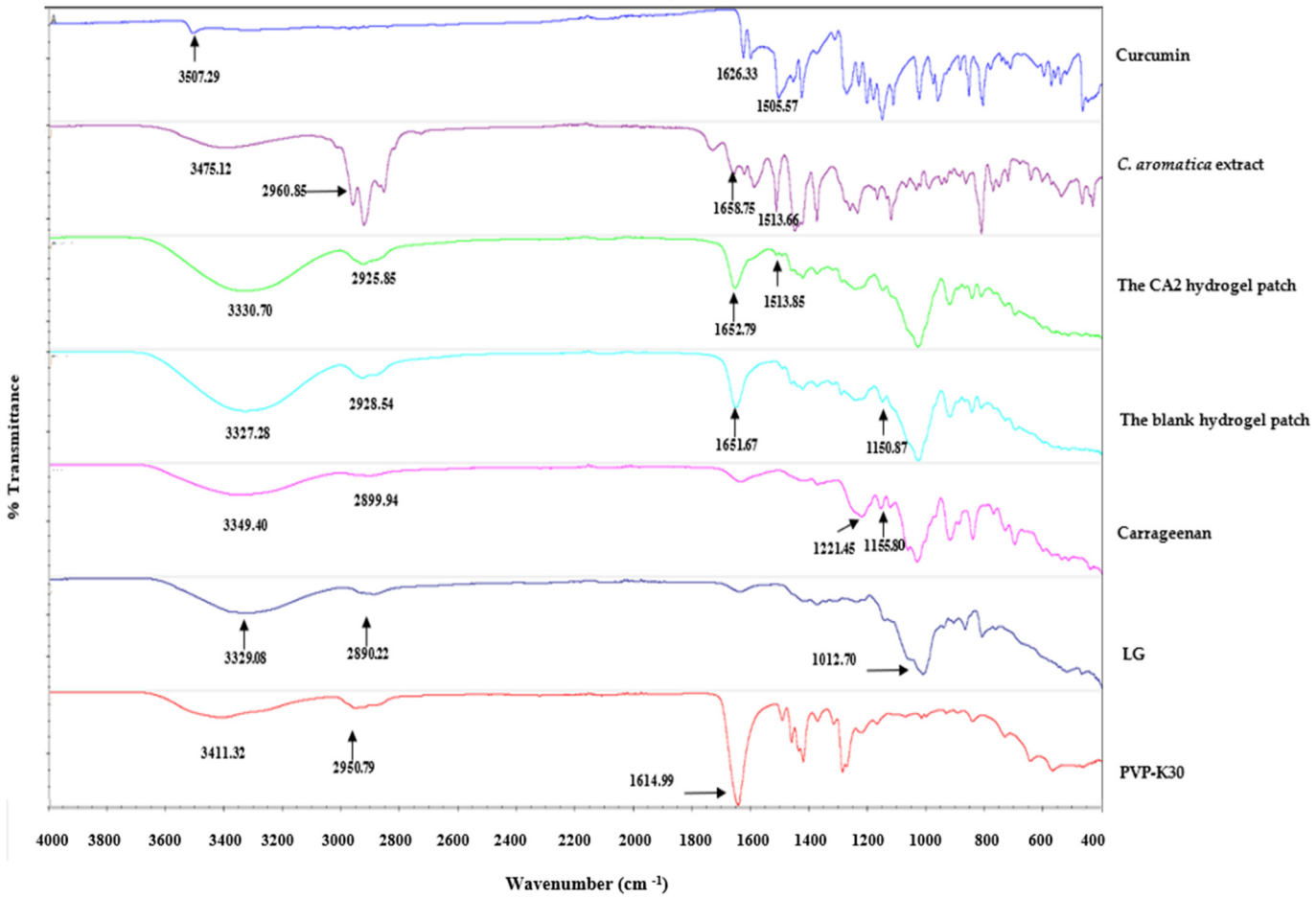


Figure 9. The FTIR spectra of curcumin, *C. aromatica* extract, the CA2 hydrogel patch, the blank hydrogel patch, carrageenan, LG, and PVP-K30.

4. Conclusions

This study revealed that the ethanolic extract of *Curcuma aromatica* (CA) had potent anti-inflammatory activity. A novel CA extract-loaded hydrogel patch was developed and demonstrated excellent physical appearance, homogeneity, and mechanical properties. The CA2 hydrogel patch reached the maximum rate of curcumin release at 12 h, and the skin permeation was sustained to 24 h. Moreover, the CA2 hydrogel patch not only showed excellent anti-inflammatory activity but also exerted anti-acne activity against *C. acnes*. The homogeneity and compatibility of all ingredients were demonstrated by its physicochemical characteristics using SEM, DSC, and XRD. The functional group of curcumin was detected by FTIR. Therefore, this study supports the traditional dermatological use of CA and indicates that the CA2 hydrogel patch showed strong cosmetic potential for

anti-inflammatory and anti-acne skincare applications. Furthermore, based on its bioactive response, the CA2 hydrogel patch may serve as a preliminary platform for future therapeutic development in dermatology, pending further studies on product stability, in vivo evaluation, and clinical investigations to confirm its safety and efficacy.

5. Patents

Thai Petty Patent Application Number 2503001915.

Author Contributions: Conceptualization, C.K.; data curation, B.O. and C.P.; Formal analysis, C.K.; Funding acquisition, C.K.; Investigation, C.K. and S.U.; Methodology, C.K. and S.U.; Resources, S.U.; Supervision, B.O. and C.P.; Visualization, C.K.; Writing—original draft, C.K.; Writing—review and editing, B.O. and C.P. All authors have read and agreed to the published version of the manuscript.

Funding: This work was supported by Walailak University under the New Researcher Development scheme (Contract Number WU67232).

Data Availability Statement: The data presented in this study are available in this article.

Acknowledgments: This work was supported by Walailak University under the New Researcher Development scheme (Contract Number WU67232). We give our thanks to Center of Excellence in Tropical Pathobiology, Walailak University, Nakhon Si Thammarat, Thailand.

Conflicts of Interest: Author C.K. is the inventor of Thai Petty Patent Application Number 2503001915. The remain authors declare that the research was conducted in the absence of any commercial or financial relationships that could be construed as a potential conflict of interest. The funders had no role in the design of the study; in the collection, analyses or interpretation of data; in the writing of the manuscript; or in the decision to publish the results.

References

1. Kowalewska, B.; Jankowiak, B.; Krajewska-Kułak, E.; Khvorik, D.F.; Niczyporuk, W. Quality of life in skin diseases as perceived by patients and nurses. *Adv. Dermatol. Allergol.* **2020**, *37*, 956–961. [CrossRef] [PubMed]
2. Chilicka, K.; Maj, J.; Panaszek, B. General quality of life of patients with acne vulgaris before and after performing selected cosmetological treatments. *Patient Prefer. Adherence* **2017**, *11*, 1357–1361. [CrossRef] [PubMed]
3. Çetinarslan, T.; Kümper, L.; Fölster-Holst, R. The immunological and structural epidermal barrier dysfunction and skin microbiome in atopic dermatitis-an update. *Front. Mol. Biosci.* **2023**, *10*, 1159404. [CrossRef]
4. Zhou, L.; Liu, X.; Li, X.; He, X.; Xiong, X.; Lai, J. Epidermal Barrier Integrity is Associated with Both Skin Microbiome Diversity and Composition in Patients with Acne Vulgaris. *Clin. Cosmet. Investig. Dermatol.* **2022**, *15*, 2065–2075. [CrossRef]
5. Bocheva, G.; Slominski, R.M.; Slominski, A.T. Environmental Air Pollutants Affecting Skin Functions with Systemic Implications. *Int. J. Mol. Sci.* **2023**, *24*, 10502. [CrossRef]
6. Cong, T.X.; Hao, D.; Wen, X.; Li, X.H.; He, G.; Jiang, X. From pathogenesis of acne vulgaris to anti-acne agents. *Arch. Dermatol. Res.* **2019**, *311*, 337–349. [CrossRef]
7. Stacey, S.K.; McEleney, M. Topical Corticosteroids: Choice and Application. *Am. Fam. Physician* **2021**, *103*, 337–343.
8. Sevimli Dikicier, B. Topical treatment of acne vulgaris: Efficiency, side effects, and adherence rate. *J. Int. Med. Res.* **2019**, *47*, 2987–2992. [CrossRef]
9. Kandhari, R. Side effects of anti-acne medications: A narrative review. *Egypt. J. Dermatol. Venereol.* **2024**, *44*, 1–6. [CrossRef]
10. Saising, J.; Maneenoon, K.; Sakulkeo, O.; Limsuwan, S.; Götz, F.; Voravuthikunchai, S.P. Ethnomedicinal Plants in Herbal Remedies Used for Treatment of Skin Diseases by Traditional Healers in Songkhla Province, Thailand. *Plants* **2022**, *11*, 880. [CrossRef]
11. Rahaman, M.M.; Rakib, A.; Mitra, S.; Tareq, A.M.; Emran, T.B.; Shahid-Ud-Daula, A.F.M.; Amin, M.N.; Simal-Gandara, J. The Genus *Curcuma* and Inflammation: Overview of the Pharmacological Perspectives. *Plants* **2021**, *10*, 63. [CrossRef]
12. Ahmed, S.; Ansari, S.H.; Ali, M.; Bhatt, D.; Ansari, F. Phytochemical and biological investigations on *Curcuma aromatica*: A review. *Pharmacogn. Rev.* **2008**, *2*, 151–156.
13. Umar, N.M.; Parumasivam, T.; Aminu, N.; Toh, S.-M. Phytochemical and pharmacological properties of *Curcuma aromatica* Salisb (wild turmeric). *J. Appl. Pharm. Sci.* **2020**, *10*, 180–194. [CrossRef]
14. Pandey, C.; Karadi, R.V.; Bhardwaj, K.L.; Sahu, K.A. Screening of selected herbal plants for anti-acne properties. *Int. J. Drug Dev. Res.* **2012**, *4*, 216–222.

15. Pabuprapap, W.; Nakyai, W.; Chaichompoo, W.; Pheedee, N.; Phetkeereerat, S.; Viyoch, J.; Yingyongnarongkul, B.; Ajavakom, V.; Chompoosor, A.; Piyachaturawat, P.; et al. *Curcuma aromatica* and *Curcuma comosa* extracts and isolated constituents provide protection against UVB-induced damage and attenuate matrix metalloproteinase-1 expression in HaCaT cells. *Cosmetics* **2022**, *9*, 23. [CrossRef]
16. Gu, J.; Sun, R.; Wang, Q.; Liu, F.; Tang, D.; Chang, X. Standardized *Astragalus mongholicus* Bunge–*Curcuma aromatica* Salisb. extract efficiently suppresses colon cancer progression through gut microbiota modification in CT26-bearing mice. *Front. Pharmacol.* **2021**, *12*, 714322. [CrossRef]
17. Pant, N.; Misra, H.; Jain, D.C.C. Phytochemical investigation of ethyl acetate extract from *Curcuma aromatica* Salisb. rhizomes. *Arab. J. Chem.* **2013**, *6*, 279–283. [CrossRef]
18. Yu, Y.; Shen, Q.; Lai, Y.; Park, S.Y.; Ou, X.; Lin, D.; Jin, M.; Zhang, W. Anti-inflammatory Effects of Curcumin in Microglial Cells. *Front. Pharmacol.* **2018**, *9*, 386. [CrossRef]
19. Benameur, T.; Soleti, R.; Panaro, M.A.; La Torre, M.E.; Monda, V.; Messina, G.; Porro, C. Curcumin as Prospective Anti-Aging Natural Compound: Focus on Brain. *Molecules* **2021**, *26*, 4794. [CrossRef]
20. Liu, C.-H.; Huang, H.-Y. In vitro anti-propionibacterium activity by curcumin containing vesicle system. *Chem. Pharm. Bull.* **2013**, *61*, 419–425. [CrossRef]
21. Zhang, Y.; Wang, D.; Liao, C.; Liu, X.; Zhang, L.; Wang, P.; Wang, X. Curcumin-mediated photodynamic therapy for mild to moderate acne: A self-controlled split-face randomized study. *Photodiagnosis Photodyn. Ther.* **2024**, *45*, 103887. [CrossRef]
22. Vollono, L.; Falconi, M.; Gaziano, R.; Iacovelli, F.; Dika, E.; Terracciano, C.; Bianchi, L.; Campione, E. Potential of Curcumin in Skin Disorders. *Nutrients* **2019**, *11*, 2169. [CrossRef] [PubMed]
23. Appendino, G.; Allegrini, P.; de Combarieu, E.; Novicelli, F.; Ramaschi, G.; Sardone, N. Shedding light on curcumin stability. *Fitoterapia* **2022**, *156*, 105084. [CrossRef] [PubMed]
24. Kharat, M.; Du, Z.; Zhang, G.; McClements, D.J. Physical and chemical stability of curcumin in aqueous solutions and emulsions: Impact of pH, temperature, and molecular environment. *J. Agric. Food Chem.* **2017**, *65*, 1525–1532. [CrossRef] [PubMed]
25. Wong, W.F.; Ang, K.P.; Sethi, G.; Looi, C.Y. Recent Advancement of Medical Patch for Transdermal Drug Delivery. *Medicina* **2023**, *59*, 778. [CrossRef]
26. Ho, T.C.; Chang, C.C.; Chan, H.P.; Chung, T.W.; Shu, C.W.; Chuang, K.P.; Duh, T.H.; Yang, M.H.; Tyan, Y.C. Hydrogels: Properties and Applications in Biomedicine. *Molecules* **2022**, *27*, 2902. [CrossRef]
27. Neamtu, B.; Barbu, A.; Negrea, M.O.; Berghea-Neamțu, C.Ș.; Popescu, D.; Zăhan, M.; Mireșan, V. Carrageenan-Based Compounds as Wound Healing Materials. *Int. J. Mol. Sci.* **2022**, *23*, 9117. [CrossRef]
28. Amruth, P.; Jacob, R.; Joy, J.M.; Visnuvinayagam, S.; Remya, S.; Mathew, S. Development of κ-carrageenan-based transparent and absorbent biodegradable films for wound dressing applications. *Int. J. Biol. Macromol.* **2024**, *282 Pt 5*, 137084. [CrossRef]
29. Zepon, K.M.; Martins, M.M.; Marques, M.S.; Heckler, J.M.; Dal Pont Morisso, F.; Moreira, M.G.; Ziulkoski, A.L.; Kanis, L.A. Smart wound dressing based on κ-carrageenan/locust bean gum/cranberry extract for monitoring bacterial infections. *Carbohydr. Polym.* **2019**, *206*, 362–370. [CrossRef]
30. Yuan, L.; Wu, Y.; Qin, Y.; Yong, H.; Liu, J. Recent advances in the preparation, characterization and applications of locust bean gum-based films. *J. Renew. Mater.* **2020**, *8*, 1565–1579. [CrossRef]
31. Kurakula, M.; Rao, G.S.N.K. Pharmaceutical assessment of polyvinylpyrrolidone (PVP): As excipient from conventional to controlled delivery systems with a spotlight on COVID-19 inhibition. *J. Drug Deliv. Sci. Technol.* **2020**, *60*, 102046. [CrossRef]
32. Patel, N.A.; Patel, N.J.; Patel, R.P. Design and evaluation of transdermal drug delivery system for curcumin as an anti-inflammatory drug. *Drug Dev. Ind. Pharm.* **2009**, *35*, 234–242. [CrossRef] [PubMed]
33. Saka, O.M.; Aygüler, C.İ.; Özdemir, N.S.; Sürücü, B.; Çakırlı, E.; Nemutlu, E.; Demirbolat, G.M. An Experimental Design Approach for Producing Curcumin-Loaded Solid Lipid Nanoparticles. *Pharmaceuticals* **2025**, *18*, 470. [CrossRef] [PubMed]
34. International Conference on Harmonisation of Technical Requirements for Registration of Pharmaceuticals for Human Use (ICH). International Conference on Harmonisation of Technical Requirements for Registration of Pharmaceuticals for Human Use. In *ICH Harmonised Tripartite Guideline: Validation of Analytical Procedures: Text and Methodology Q2(R1)*; ICH: Geneva, Switzerland, 2005; pp. 6–13.
35. Kongkwamcharoen, C.; Itharat, A.; Ketjinda, W.; Lee, H.Y.; Moon, G.S.; Davies, N.M. Formulation design and physicochemical evaluation of an anti-inflammatory hydrogel patch containing *Crinum asiaticum* L. extract. *Res. Pharm. Sci.* **2023**, *18*, 244–261. [CrossRef]
36. Proksch, E. pH in nature, humans and skin. *J. Dermatol.* **2018**, *45*, 1044–1052. [CrossRef]
37. Berg, R.W.; Milligan, M.C.; Sarbaugh, F.C. Association of skin wetness and pH with diaper dermatitis. *Pediatr. Dermatol.* **1994**, *11*, 18–20. [CrossRef]
38. Blaak, J.; Staib, P. The Relation of pH and Skin Cleansing. *Curr. Probl. Dermatol.* **2018**, *54*, 132–142. [CrossRef]
39. Prakash, C.; Bhargava, P.; Tiwari, S.; Majumdar, B.; Bhargava, R.K. Skin Surface pH in Acne Vulgaris: Insights from an Observational Study and Review of the Literature. *J. Clin. Aesthetic Dermatol.* **2017**, *10*, 33–39.

40. Syed, M.S.; Azam, F.; Ahmad, S.; Ahmad, F.; Mushtaq, B.; Habib, S.; Rasheed, A.; Zafar, M.S.; Rasul, S. Development of environment friendly biodegradable biopolymer-based hydrogel composites incorporated with waste cotton for wound dressings. *J. Ind. Text.* **2025**, *55*, 15280837251324895. [CrossRef]
41. Musa, I.; Rotaru-Zavaleanu, A.D.; Sfredel, V.; Aldea, M.; Gresita, A.; Glavan, D.G. Post-Stroke Recovery: A Review of Hydrogel-Based Phytochemical Delivery Systems. *Gels* **2025**, *11*, 260. [CrossRef]
42. Petitjean, M.; Isasi, J.R. Locust Bean Gum, a Vegetable Hydrocolloid with Industrial and Biopharmaceutical Applications. *Molecules* **2022**, *27*, 8265. [CrossRef] [PubMed]
43. Lomartire, S.; Gonçalves, A.M.M. Algal Phycocolloids: Bioactivities and Pharmaceutical Applications. *Mar. Drugs* **2023**, *21*, 384. [CrossRef]
44. Tako, M.; Nakamura, S. Synergistic interaction between kappa-carrageenan and locust-bean gum in aqueous media. *Agric. Biol. Chem.* **1986**, *50*, 2817–2822. [CrossRef]
45. Martins, J.T.; Cerqueira, M.A.; Bourbon, A.I.; Pinheiro, A.C.; Souza, B.W.S.; Vicente, A.A. Synergistic effects between κ-carrageenan and locust bean gum on physicochemical properties of edible films made thereof. *Food Hydrocoll.* **2012**, *29*, 280–289. [CrossRef]
46. Ballesteros-Mártinez, L.; Pérez, C.E.; Andrade, R. Effect of glycerol and sorbitol concentrations on mechanical, optical, and barrier properties of sweet potato starch film. *NFS J.* **2020**, *20*, 1–9. [CrossRef]
47. Kaur, R.; Sharma, A.; Puri, V.; Singh, I. Preparation and characterization of biocomposite films of carrageenan/locust bean gum/montmorrillonite for transdermal delivery of curcumin. *BioImpacts BI* **2019**, *9*, 37–43. [CrossRef]
48. Coondoo, A.; Phiske, M.; Vermah, S.; Lahiri, K. Side-effects of topical steroids: A long overdue revisit. *Indian Dermatol. Online J.* **2014**, *5*, 416–425. [CrossRef]
49. Pintatum, A.; Maneerat, W.; Logie, E.; Tuenter, E.; Sakavitsi, M.E.; Pieters, L.; Berghe, W.V.; Sripisut, T.; Deachathai, S.; Laphookhieo, S. In Vitro Anti-Inflammatory, Anti-Oxidant, and Cytotoxic Activities of Four *Curcuma* Species and the Isolation of Compounds from *Curcuma aromatica* Rhizome. *Biomolecules* **2020**, *10*, 799. [CrossRef]
50. Kim, H.; Hong, J.; Lee, J.; Jeon, W.; Yeo, C.; Lee, Y.; Baek, S.; Ha, I. *Curcuma aromatica* Salisb. Protects from Acetaminophen-Induced Hepatotoxicity by Regulating the Sirt1/HO-1 Signaling Pathway. *Nutrients* **2023**, *15*, 808. [CrossRef]
51. Peng, Y.; Ao, M.; Dong, B.; Jiang, Y.; Yu, L.; Chen, Z.; Hu, C.; Xu, R. Anti-Inflammatory Effects of Curcumin in the Inflammatory Diseases: Status, Limitations and Countermeasures. *Drug Des. Dev. Ther.* **2021**, *15*, 4503–4525. [CrossRef]
52. Feldman, S.R.; Chen, D.M. How patients experience and manage dryness and irritation from acne treatment. *J. Drugs Dermatol. JDD* **2011**, *10*, 605–608.
53. Kwon, K.C.; Won, J.G.; Kim, M.S.; Shin, Y.W.; Park, S.W.; Song, Y.S. Anti-acne activity of carnitine salicylate and magnolol through the regulation of exfoliation, lipogenesis, bacterial growth and inflammation. *Skin Res. Technol.* **2023**, *29*, e13406. [CrossRef]
54. Wang, R.; Cheng, C.; Wang, H.; Wang, D. Swollen hydrogel nanotechnology: Advanced applications of the rudimentary swelling properties of hydrogels. *ChemPhysMater* **2024**, *3*, 357–375. [CrossRef]
55. Gounden, V.; Singh, M. Hydrogels and Wound Healing: Current and Future Prospects. *Gels* **2024**, *10*, 43. [CrossRef] [PubMed]
56. Abdallah, M.H.; Shahien, M.M.; El-Horany, H.E.-S.; Ahmed, E.H. Modified Phospholipid Vesicular Gel for Transdermal Drug Delivery: The Influence of Glycerin and/or Ethanol on Their Lipid Bilayer Fluidity and Penetration Characteristics. *Gels* **2025**, *11*, 358. [CrossRef] [PubMed]
57. Liew, J.W.Y.; Loh, K.S.; Ahmad, A.; Lim, K.L.; Wan Daud, W.R. Synthesis and characterization of modified κ-carrageenan for enhanced proton conductivity as polymer electrolyte membrane. *PLoS ONE* **2017**, *12*, e0185313. [CrossRef]
58. Elnashar, M.M.; Yassin, M.A. Lactose hydrolysis by beta-galactosidase covalently immobilized to thermally stable biopolymers. *Appl. Biochem. Biotechnol.* **2009**, *159*, 426–437. [CrossRef]
59. Kamaly, N.; Yameen, B.; Wu, J.; Farokhzad, O.C. Degradable Controlled-Release Polymers and Polymeric Nanoparticles: Mechanisms of Controlling Drug Release. *Chem. Rev.* **2016**, *116*, 2602–2663. [CrossRef]
60. Febriyenti Indra, P.; Zaini, E.; Ismed, F.; Lucida, H. Preparation and characterization of quercetin-polyvinylpyrrolidone K-30 spray dried solid dispersion [Preparación y caracterización de dispersión sólida de quercetina-polivinilpirrolidona K-30 secada por rociado]. *J. Pharm. Pharmacogn. Res.* **2020**, *8*, 127–134. [CrossRef]
61. Wdowiak, K.; Tajber, L.; Miklaszewski, A.; Cielecka-Piontek, J. Sweeteners Show a Plasticizing Effect on PVP K30—A Solution for the Hot-Melt Extrusion of Fixed-Dose Amorphous Curcumin-Hesperetin Solid Dispersions. *Pharmaceutics* **2024**, *16*, 659. [CrossRef]
62. Hezma, A.M.; Abdelrazzak, A.B.; El-Bahy, G.S. Preparation and spectroscopic investigations of hydroxyapatite-curcumin nanoparticles-loaded polylactic acid for biomedical application. *Egypt. J. Basic Appl. Sci.* **2019**, *6*, 1–9. [CrossRef]
63. Anand, R.; Collard, D.; Thomann, J.S.; Duday, D. Antimicrobial Sponge: A Polyvinyl Alcohol, Tannic Acid and Curcumin-Loaded Nanolignin Hydrogel Composite Scaffold. *Gels* **2025**, *11*, 168. [CrossRef]

Disclaimer/Publisher's Note: The statements, opinions and data contained in all publications are solely those of the individual author(s) and contributor(s) and not of MDPI and/or the editor(s). MDPI and/or the editor(s) disclaim responsibility for any injury to people or property resulting from any ideas, methods, instructions or products referred to in the content.